Poster presented at the
Cool Stars 13 workshop, 2004-07-05..09, Hamburg, Germany

Synthetic line profiles from numerical simulations of a red supergiant

Bernd Freytag[1,2]
Michelle Mizuno-Wiedner[2]
Bengt Gustafsson[2]

1: GRAAL, Université de Montpellier II, France
2: Department for Astronomy and Space Physics at Uppsala University, Sweden

Abstract

Radiation hydrodynamics simulations of the outer envelope and the atmosphere of a red supergiant (like Betelgeuse) have been performed with CO^{5}BOLD. The resulting models reveal a variety of surface features that can be attributed to small surface and large envelope convection cells, to pressure fluctuations in the stellar interior and shock waves in the atmosphere.

In this poster we demonstrate the relation between the local temperature and velocity stratifications and (spatially and temporally resolved) intensity line profiles calculated from them. Furthermore, we discuss the temporal variations of the flux profiles and compare with observations by Gray.

Models and synthetic spectra of Betelgeuse

The parameters of the red supergiant Betelgeuse (M1-2 Ia-Iab) are not very well known:

- Θ=42 – 65 mas, R=600 – 1000 $R_\odot$
- Hipparcos-distance =131 $\pm$ 30 pc
- M=5 – 20 $M_\odot$, $T_{\rm eff}$=3400 – 3600 K

To model the outer layers of Betelgeuse the code CO^{5}BOLD has been used. It numerically integrates the coupled non-linear equations of compressible hydrodynamics and non-local radiation transport on a Cartesian grid. It accounts for ionization effects and realistic (grey) opacities. The parameters (especially the rather low mass) for the presented model were chosen to favor large convective cells to make it easier to resolve them on a given numerical grid. Parameters for model st35gm04n29:

- Computational domain: cube, edge length 1626 $R_\odot$, 235^3 grid points
- Gravitation: spherical $1/r$ potential, smoothed in the center
- $M_\star = 5 M_\odot$
- $T_{\rm eff} \sim$ 3330 K, $\log g \sim$ -0.46 (cgs units)
- $R_\star \sim 630\, R_\odot$, $L_\star \sim 42\,000\, L_\odot$

Post-processing: spectrum synthesis for a single line for 67 snapshots:

- Fe I
- λ=6219.281 Å, excitation energy=2.198 eV
- Simulation time: 4.2 years

Observations

The irregular lightcurve of Betelgeuse (Goldberg, L., 1984, PASP 96, 366), interferometric detections of hot-spots in the optical (e.g. Buscher et al., 1990, MNRAS 245, 7p; Burns et al., 1997, MNRAS 290, L11, Young et al., 2000, MNRAS 315, 635), and inhomogeneities in the atmosphere (VLA observations: Lim et al., 1998, Nature 392, 575) or chromosphere (with HST: Gilliland, L., Dupree, A.K., 1996, ApJ 463, L29) favor a picture of the near-surface layers which large-scale structures and violent motions.

Based on simple scaling arguments Schwarzschild suggested in 1975 (ApJ 195, 137) that a few giant convective cells on the surface of Betelgeuse are the cause for the observed temporal brightness variations.

However, Gray (2000, ApJ 532, 487; 2001, PASP 113, 1378) has argued that the stability of photospheric line profiles in the spectrum of Betelgeuse (M1-2 Ia-Iab) suggests that the stellar photosphere is not characterised by the presence of a few giant convection cells, contrary to what is proposed by the 3D radiation hydrodynamics simulations of Freytag (see Freytag, B., Steffen, M., Dorch, B., 2002, Astron. Nachr. 323, 213).

Observed versus synthetic line profiles

We have used a simulated 3D models to calculate the time variations of a number of spectral lines. Here, we display the resulting profile variations of the Fe I λ6219 line (examples for spatially resolved lines can be found in Figs. 7 to 14).

For this line, Gray found continuum depth variation by typically $\pm$20% and a half width of about 25 km/s, varying between 23.5 km/s and 27 km/s over 17 months (with large gaps resulting in about 11 months effective coverage). However, the normalized line profile variations were at the most on the order of 2% in rest intensity, which was interpreted as "additional blend" and not as temporary bumps in the profiles that were thought to result from giant convection cells.

As is seen in Fig. 1, the variations in core line depth of our calculated profiles are similar to those found by Gray. The variations in half-width, however, are significantly greater than those observed by Gray, as seen in Fig. 2: the full width at half line depth varies by almost a factor of two, from 12 km/s to 23 km/s over 4 years, with an average of about 17 km/s. The reason for this is that the line profile of the simulations show systematically much larger profile variations than those observed, as is shown by the sample of line profile variations shown in Figs. 5 and 6.

However, the 11 (or even 17) months of Gray's observations are not sufficient to derive precise results about the statistics of profile variations of Betelgeuse. E.g., it is easily possible to find a window of 17 months in the plot of the variations of the half-width of the synthetic lines (Fig. 2) that has a smaller amplitude (in km/s) than the observed ones.

The smoothness of the synthetic profiles agrees well with the observations in Gray (2001). There is no trace of the fine-structured cores Gray found in earlier observations (2000).

Conclusions

Taking into account the instrumental profile (with a resolution of about 3 km/s in Grays observations) and especially the broadening of lines by blends in the spectrum synthesis would reduce the amplitude of the variation of the half-width somewhat and move the mean value closer to the observed one.

However, the variations would still be larger than in the observations, supporting the conclusion that the number of convective elements on Betelgeuse is greater than what is predicted by the present simulations.

Extrapolating the results of the current model with 5 solar masses to a (not yet existing) 10 solar mass model with the same radius would lead to about 4 times the number of surface cells and approximately half the amplitude of the variations. This simple (but computationally very demanding) adjustment of the model mass towards a more likely value for a red supergiant may bring simulations and observations into agreement – in the limits set by the complex behavior of Betelgeuse and the small time spans of data available.

Line core depth and half-width over time

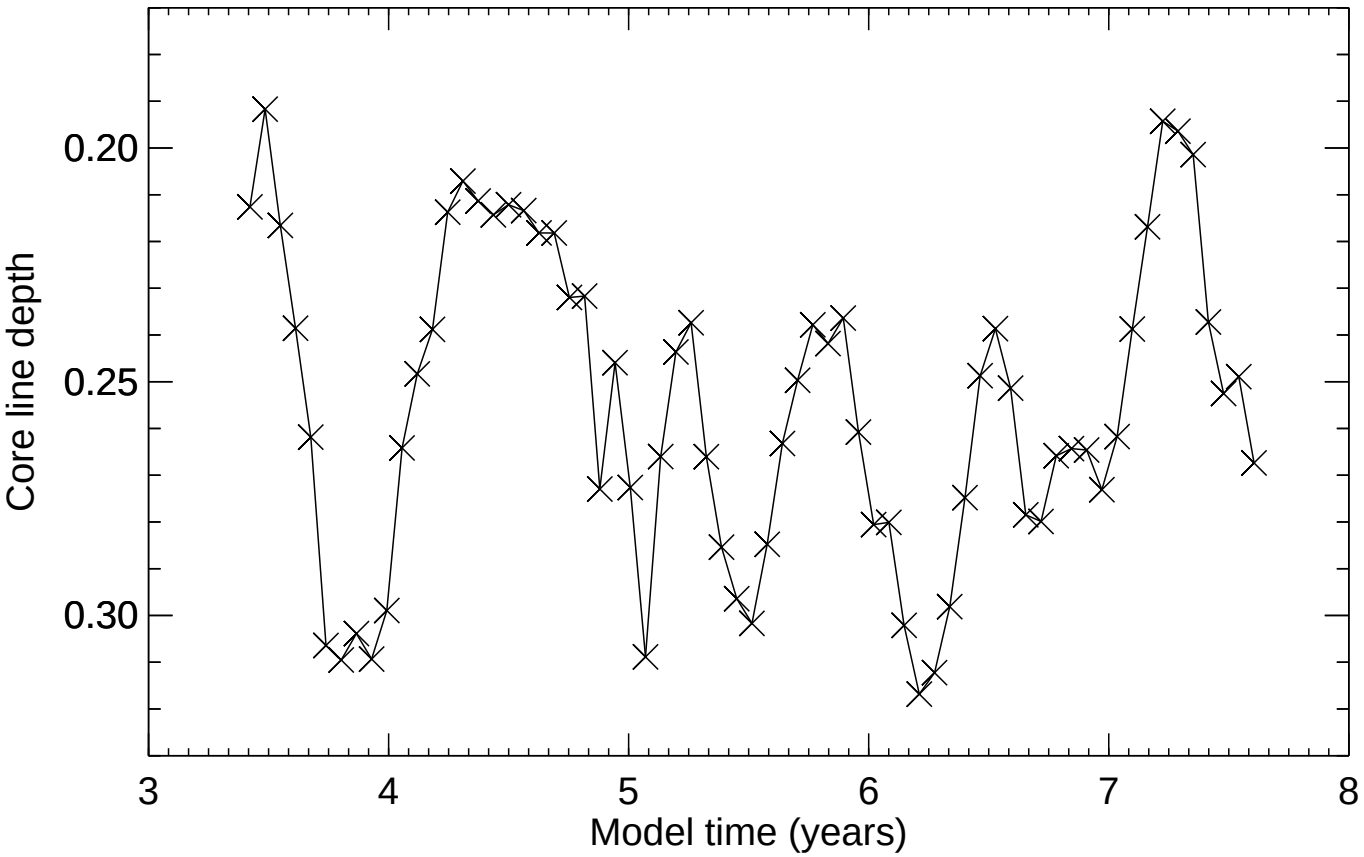

Figure 1: Line core depth variations over 4.2 years model time.

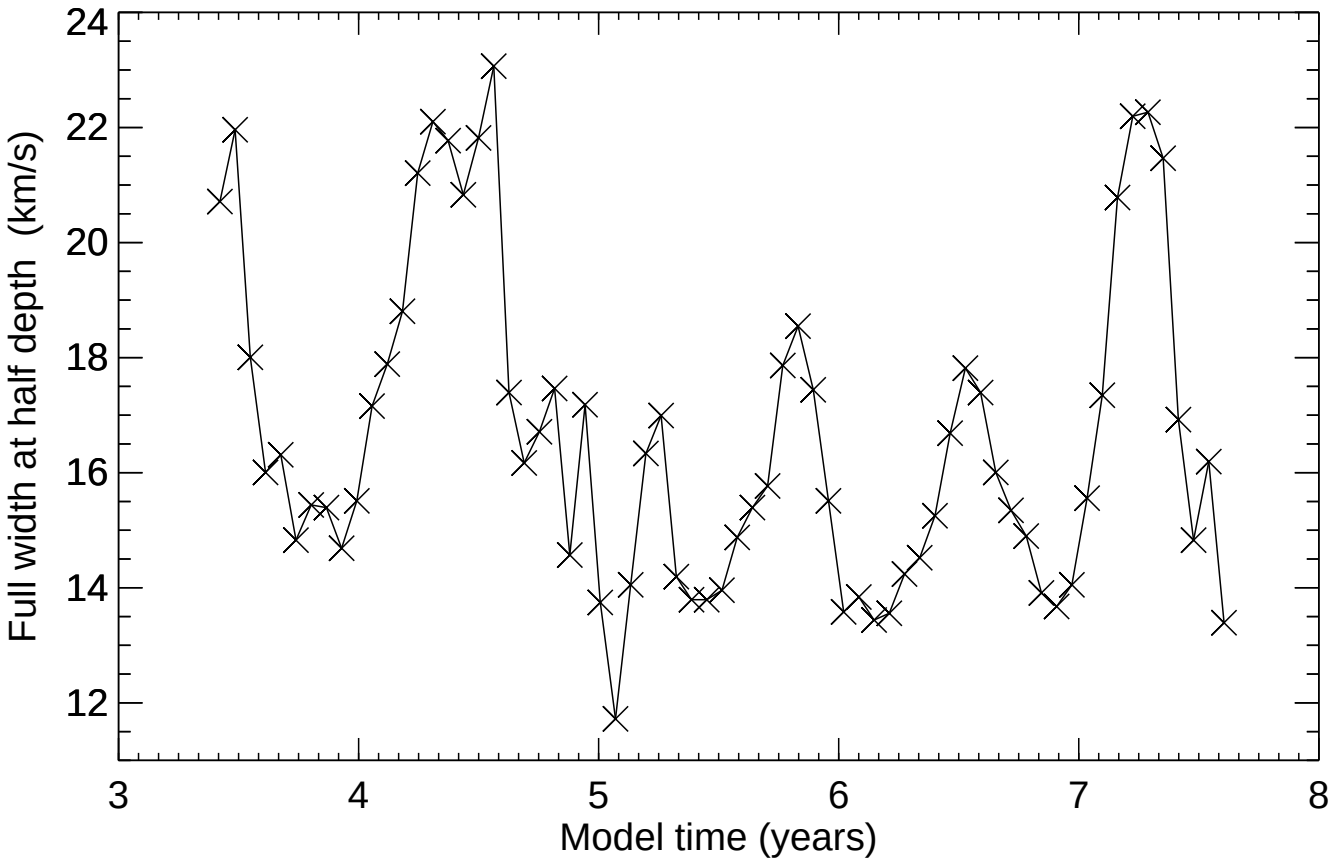

Figure 2: Variations of line width over 4.2 years model time.

Continuum level and line core shift over time

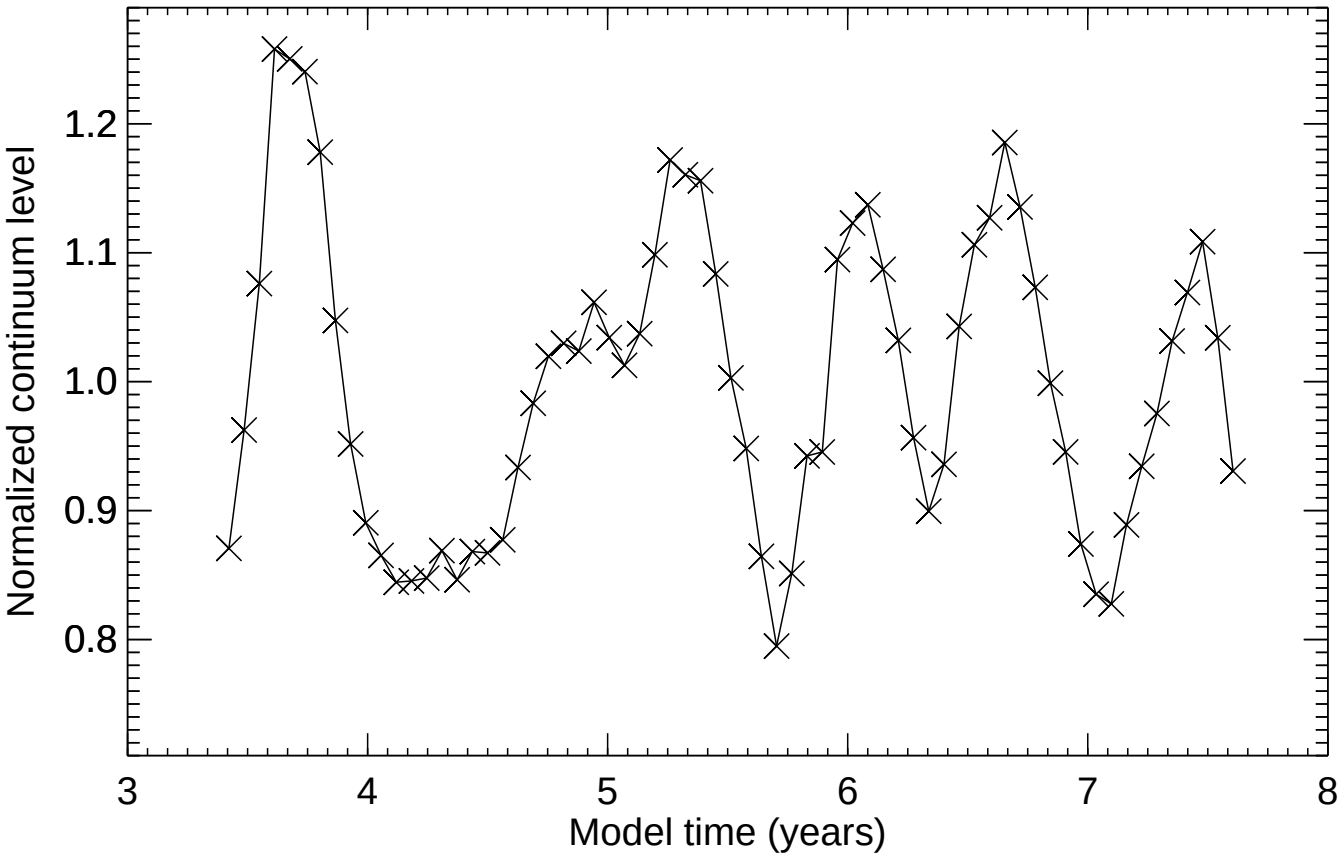

Figure 3: Variations of continuum level over 4.2 years model time.

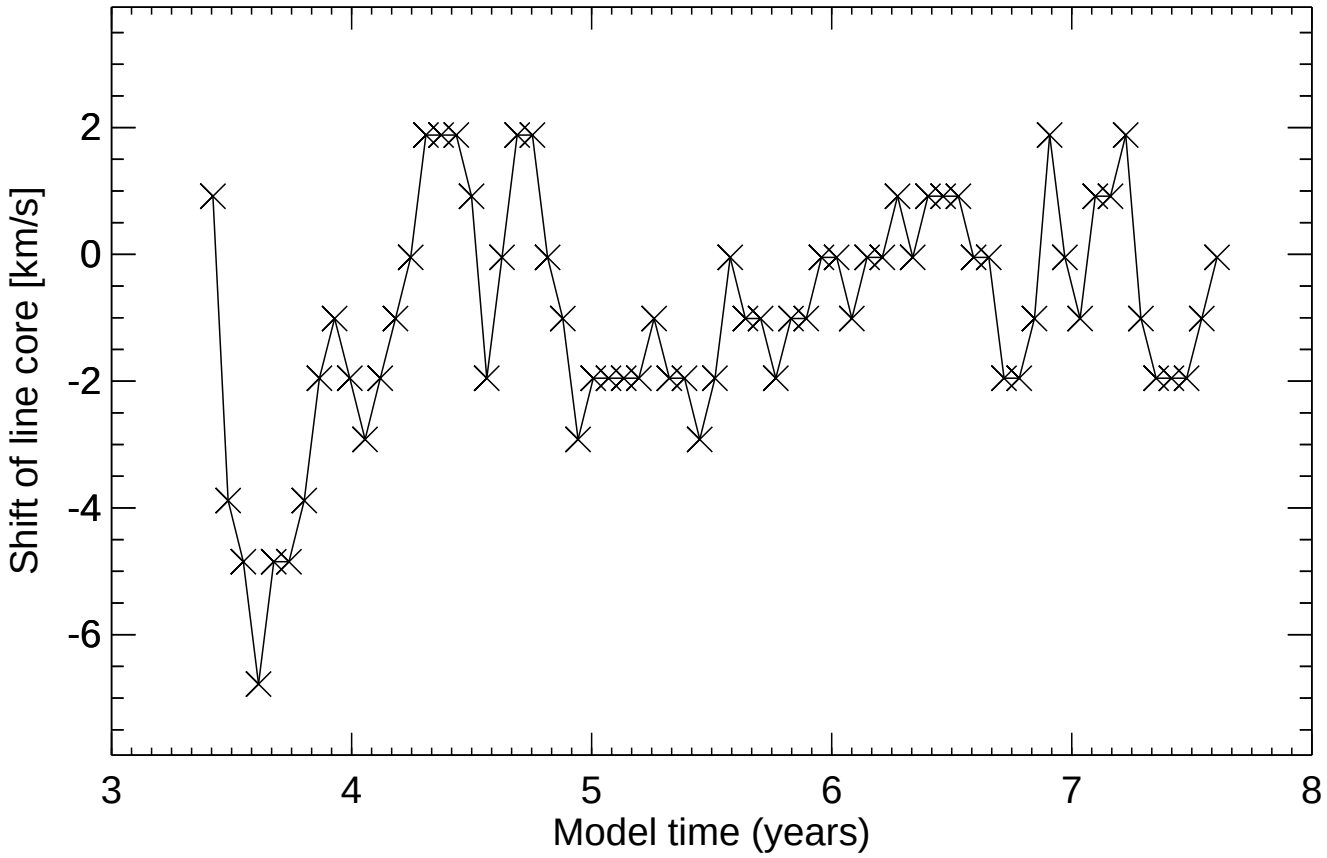

Figure 4: Variations of position of line core over 4.2 years model time (from wavelength at minimum flux).

Line profile variation over time

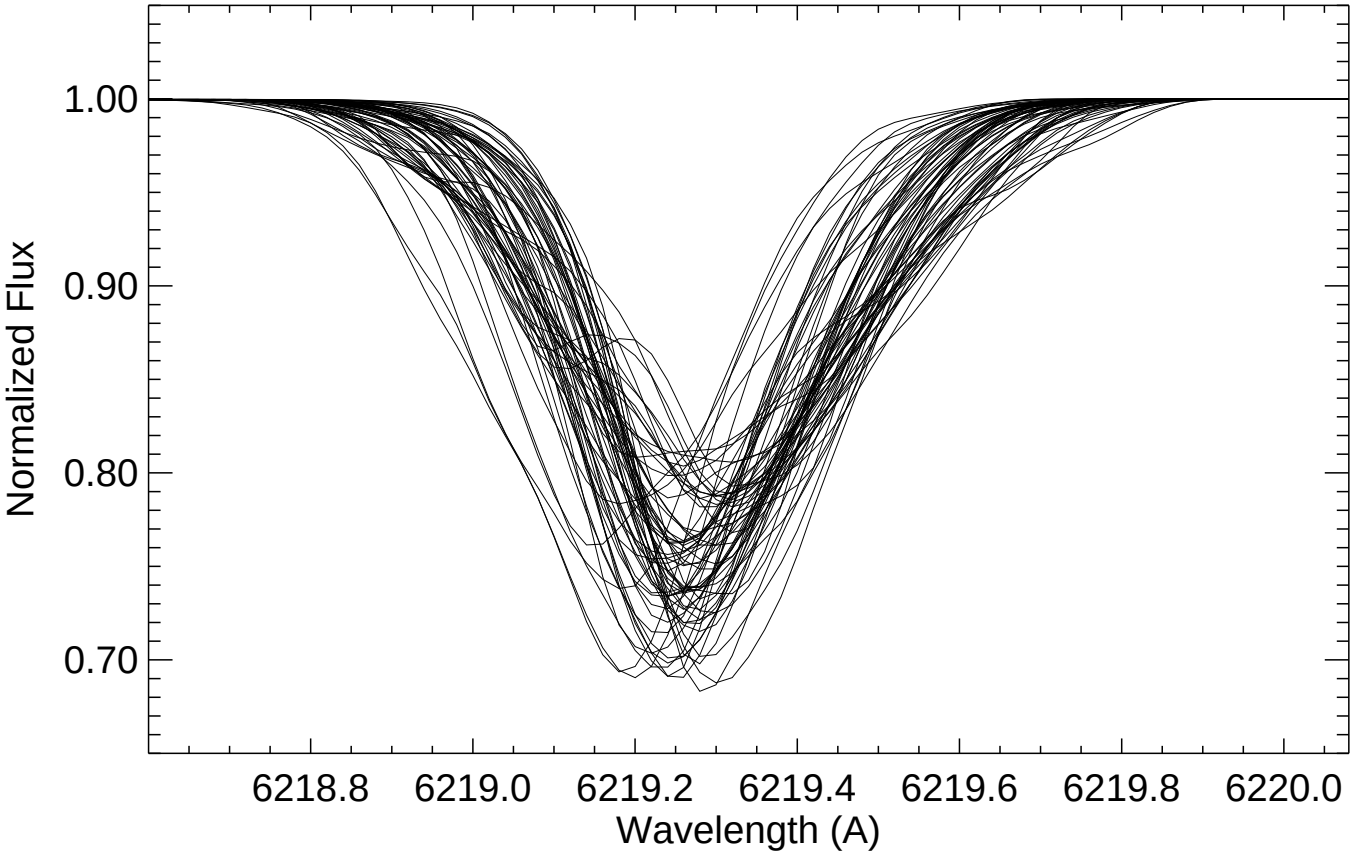

Figure 5: Variations of line profiles over 4.2 years model time.

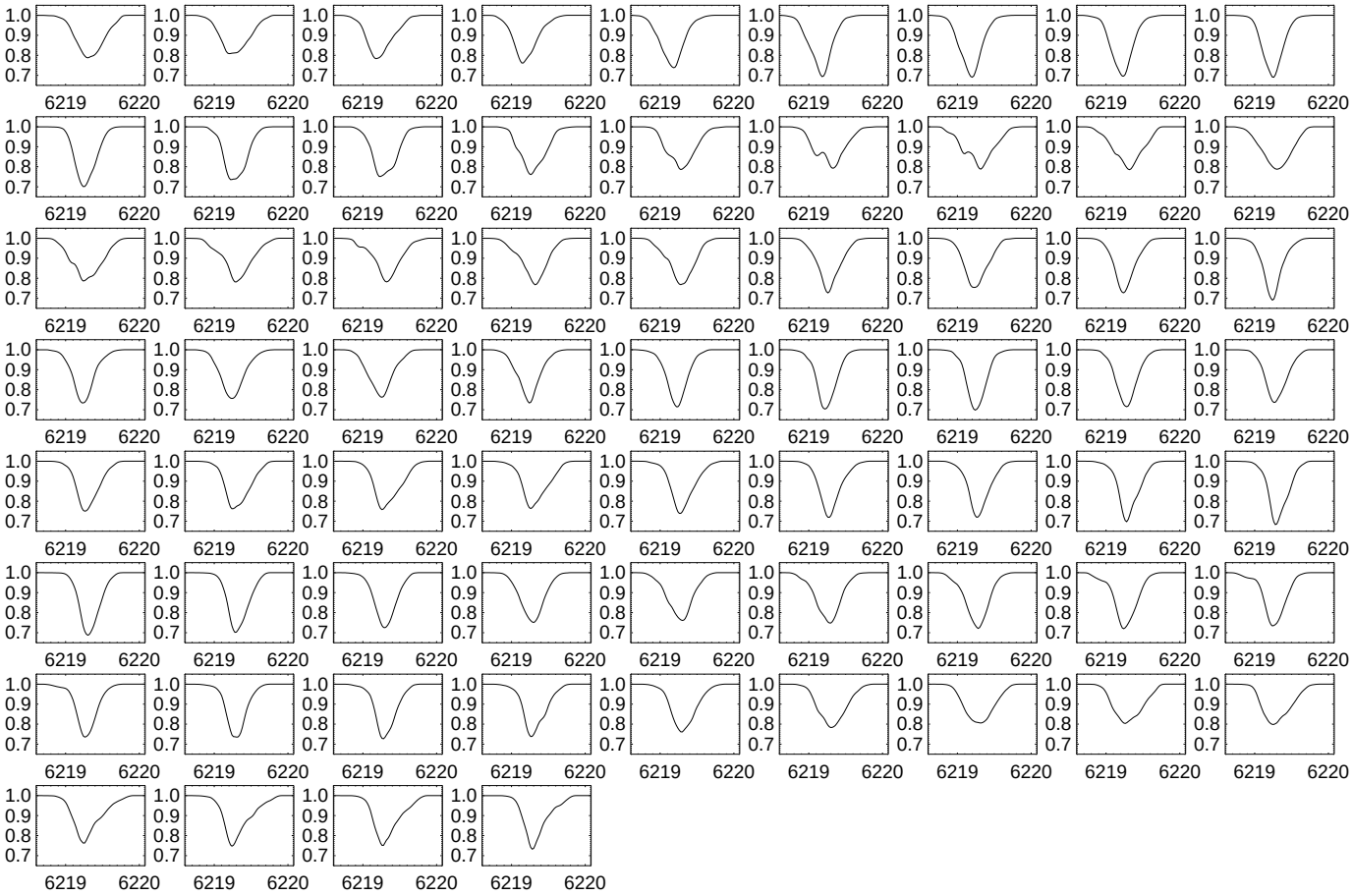

Figure 6: Variations of line profiles over 4.2 years model time. Profile 35 is selected as "snapshot 1", profile 15 is "snapshot 2" in the following figures.

Line profile of snapshot 1

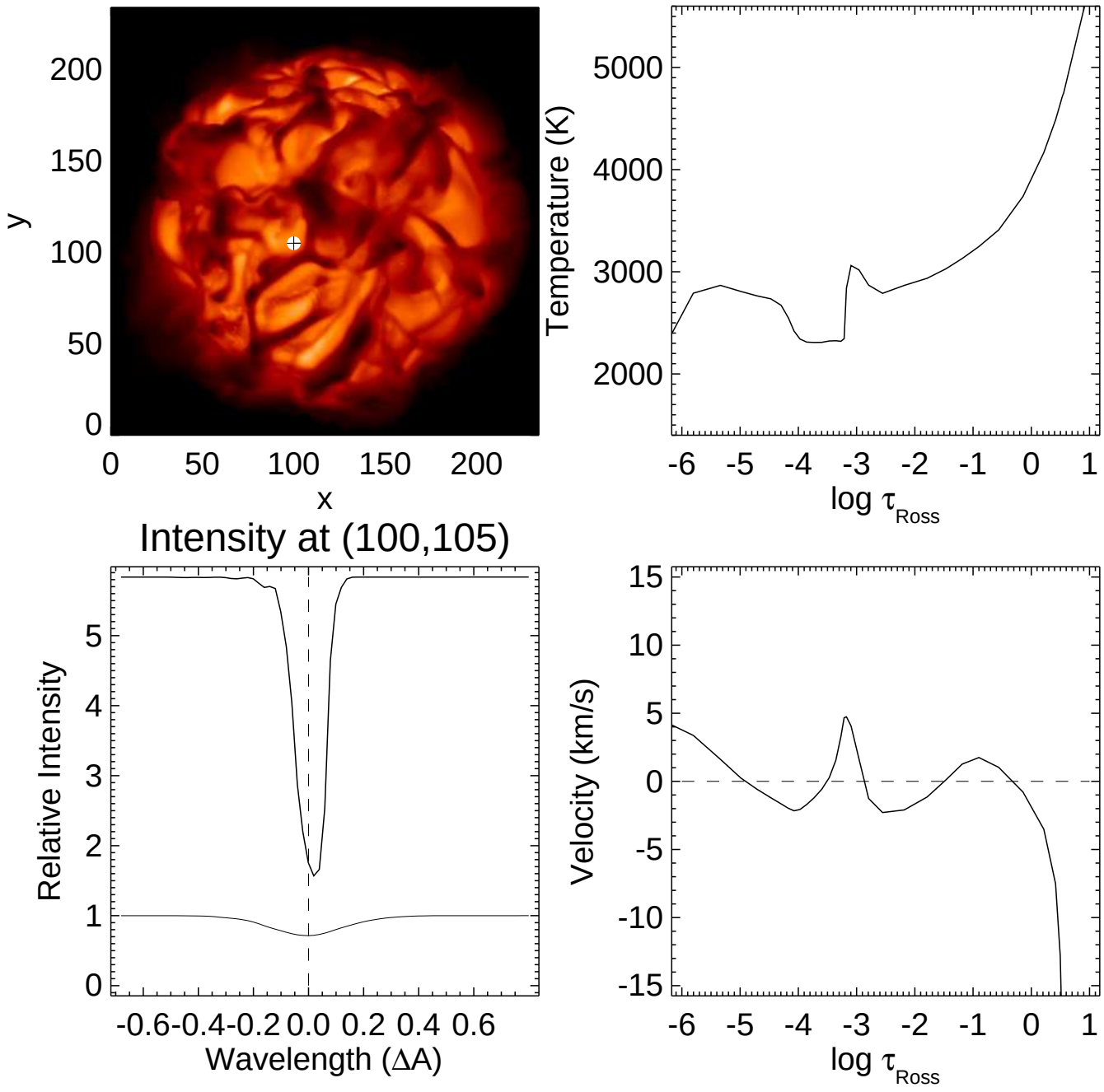

Figure 7: Sample line profile around 6219.281 Å: Upper left: continuum image with mark at the point from which the spectrum is taken. Upper right: temperature over logarithm of Rosseland optical depth. Lower left: thick line: sample spectrum over wavelength shift relative to λ=6219.281 Å; thin line: disk integrated spectrum with continuum normalized to one. Lower right: velocity along line of sight. This narrow profile is taken from a bright granule where the stratification shows rather small velocity fluctuations.

Line profile of snapshot 1

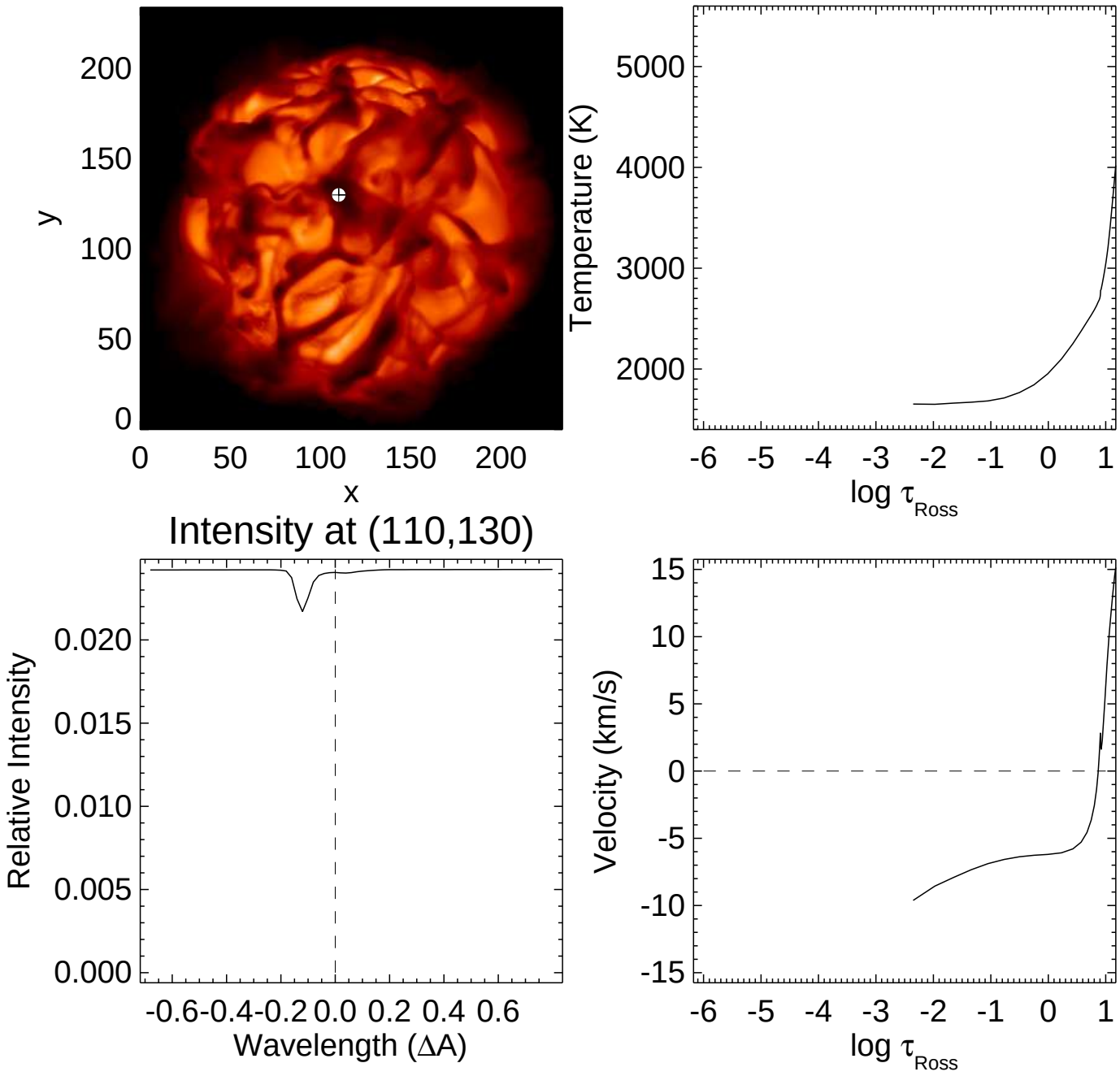

Figure 8: Sample line profile around 6219.281 Å: see Fig. 7. This profile is taken from a dark region with an intensity about a factor 50 lower than the "granule intensity".

Line profile of snapshot 1

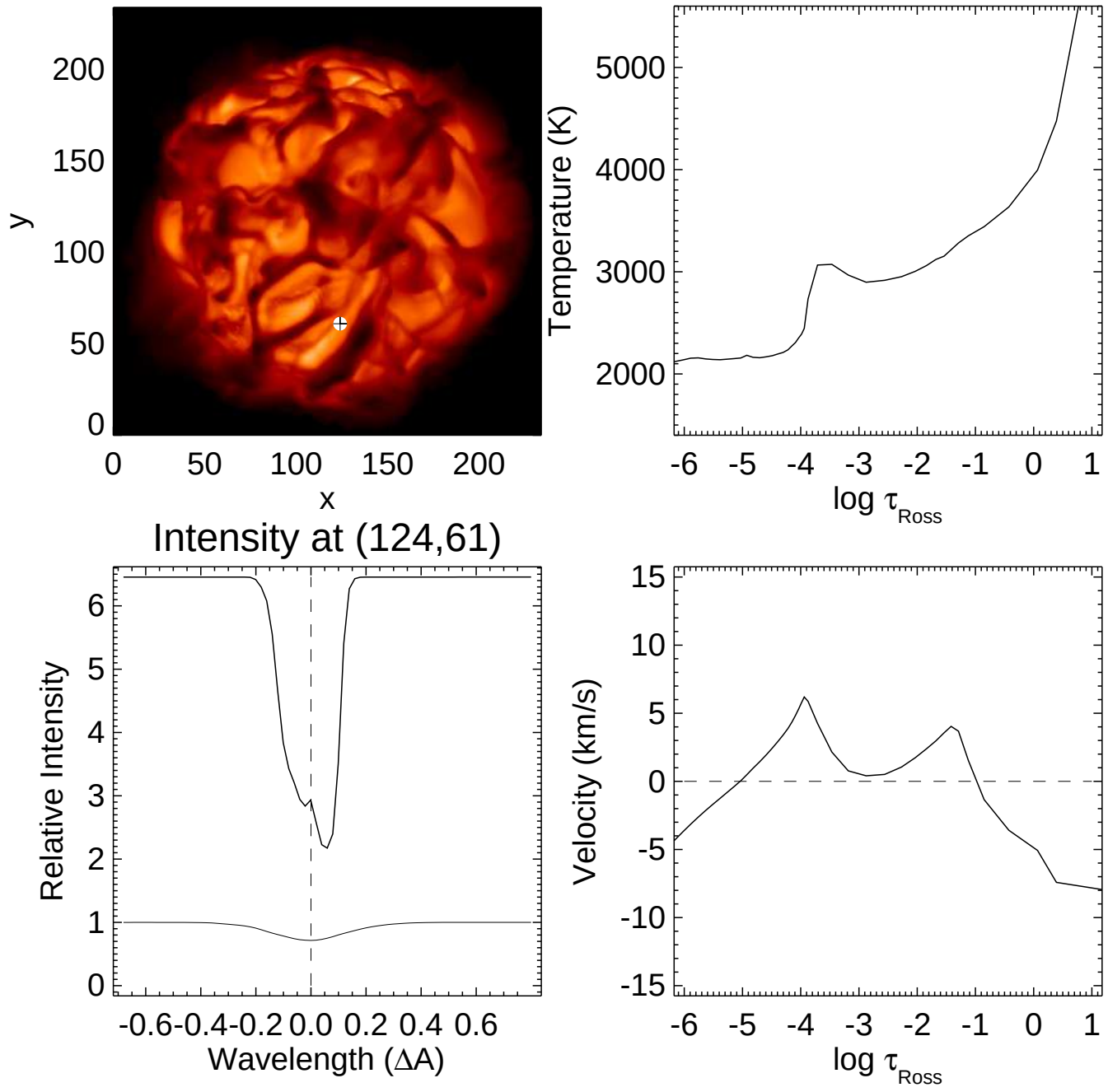

Figure 9: Sample line profile around 6219.281 Å: see Fig. 7. A bright area with a double bump profile.

Line profile of snapshot 1

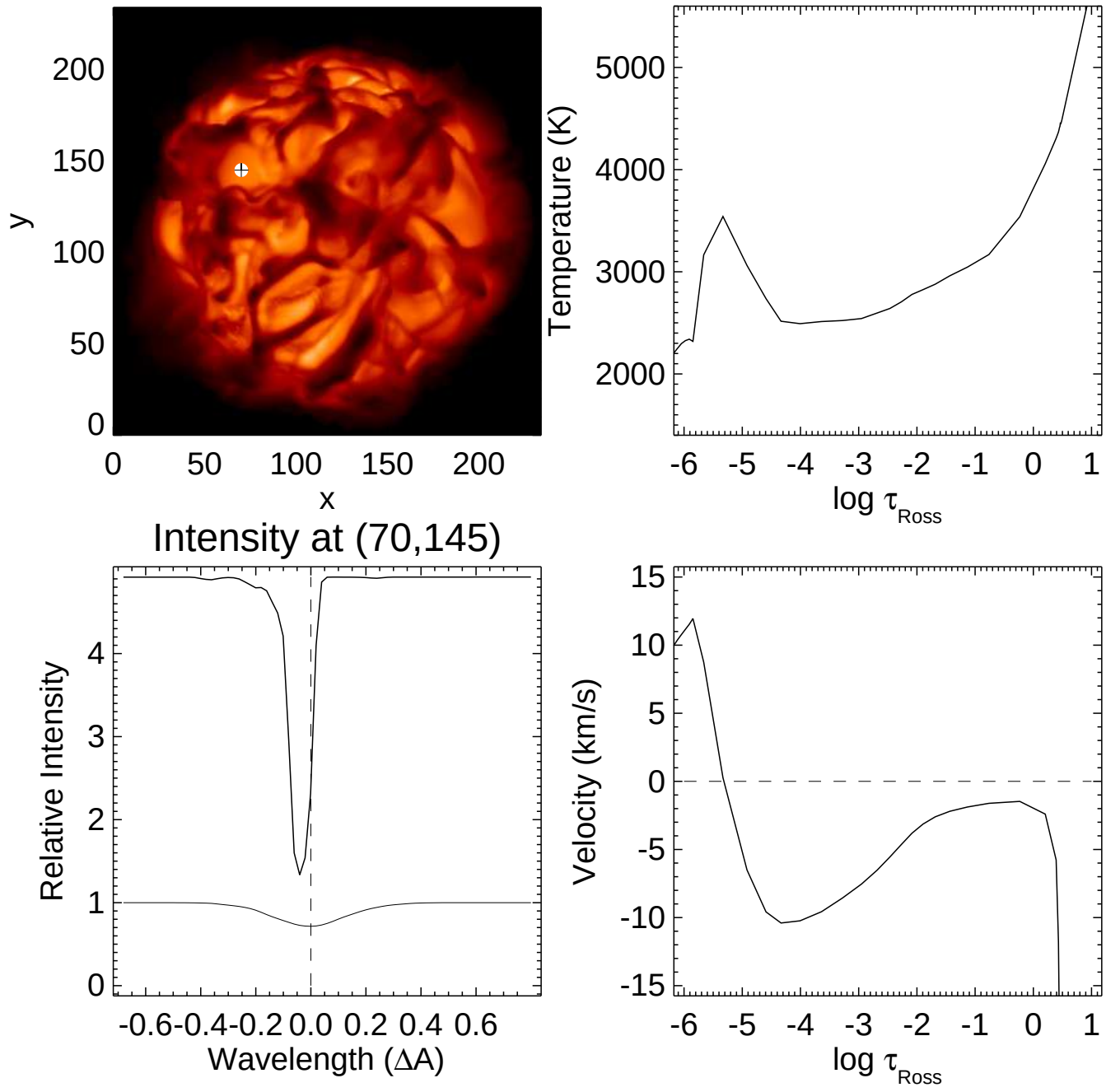

Figure 10: Sample line profile around 6219.281 Å: see Fig. 7. A "granule profile" with a net blue-shift.

Line profile of snapshot 1

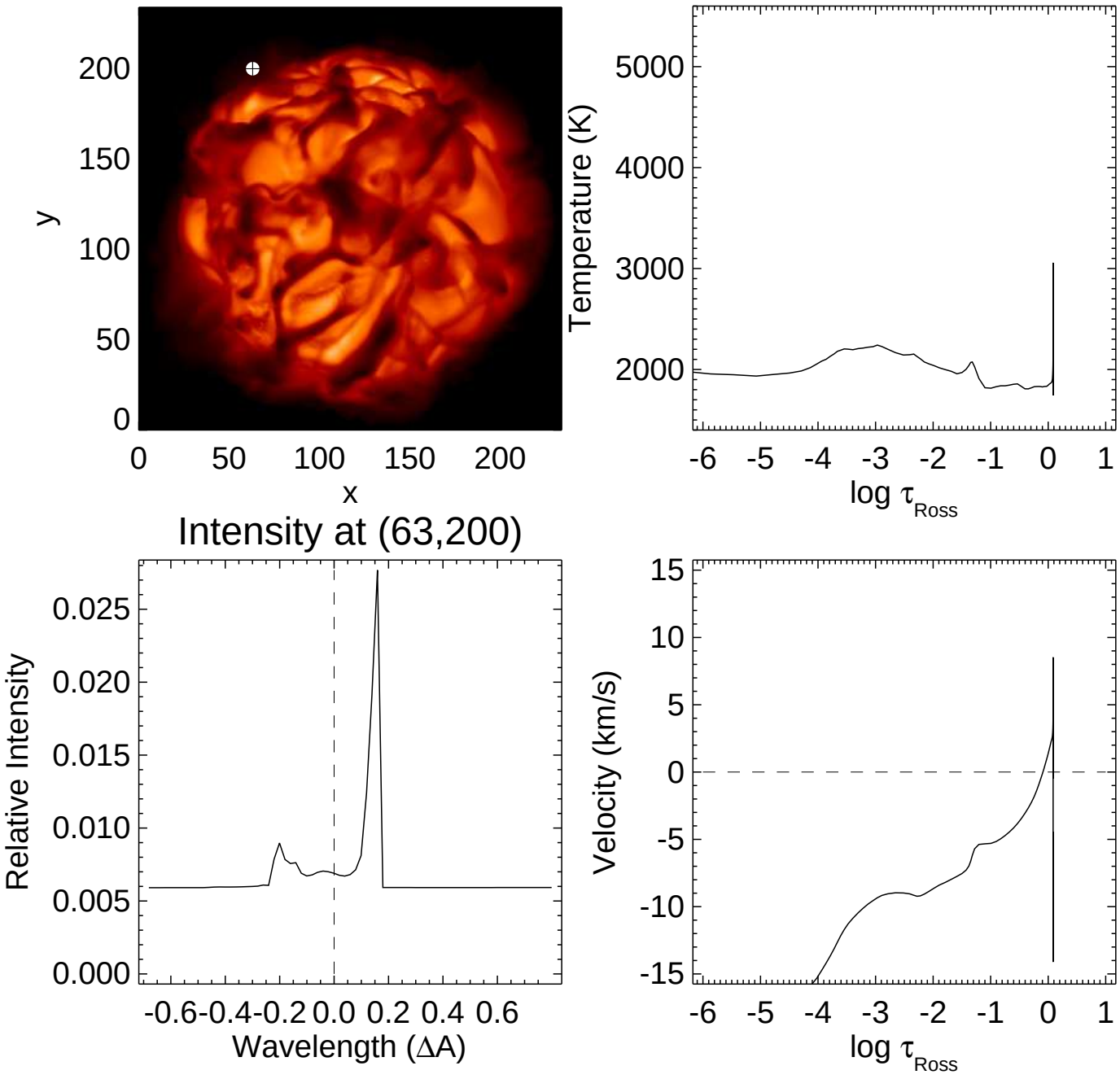

Figure 11: Sample line profile around 6219.281 Å: see Fig. 7. Emission line from the limb. The entire Rosseland optical thickness of that column is just above one.

Line profile of snapshot 2

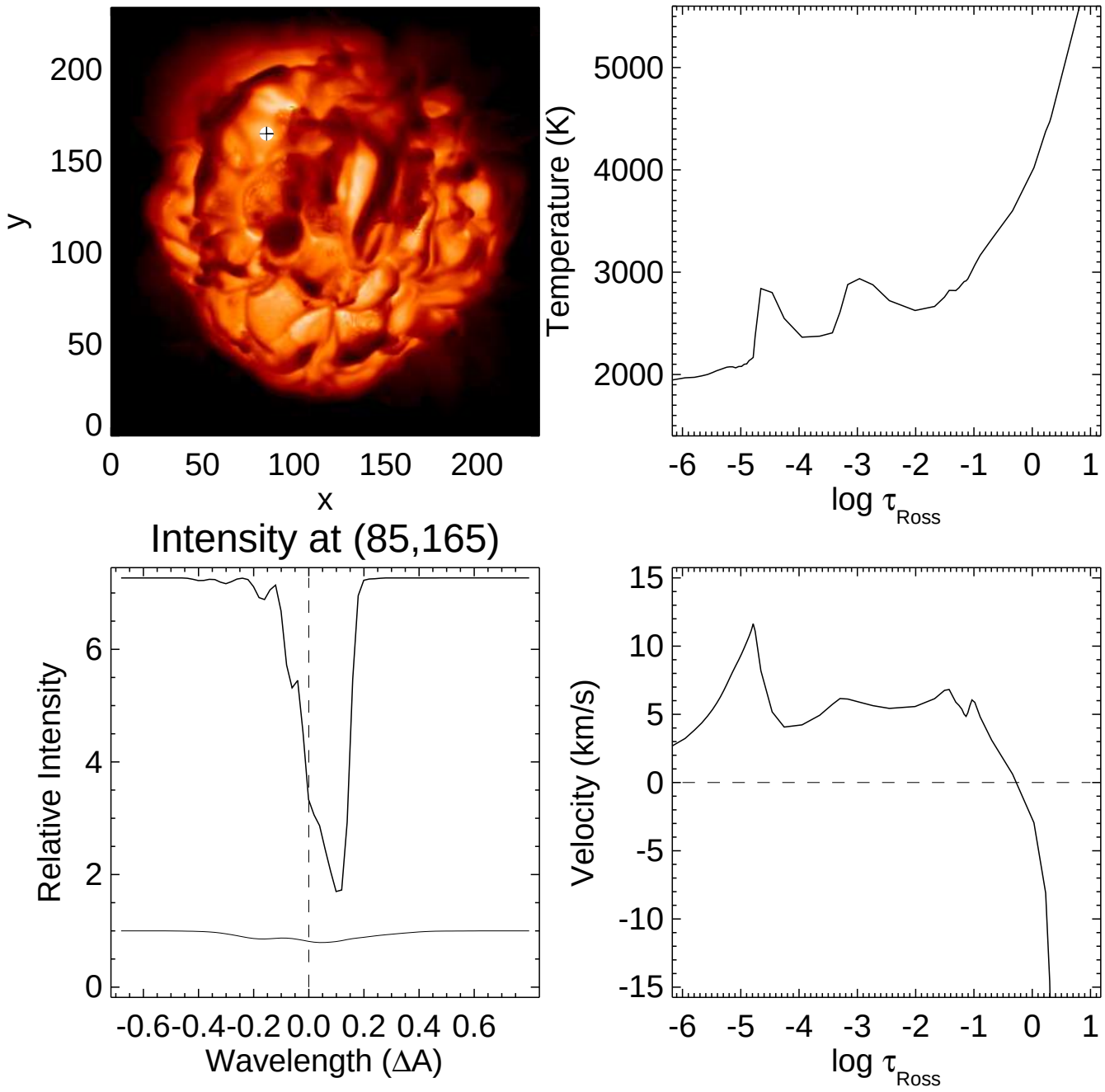

Figure 12: Sample line profile around 6219.281 Å: see Fig. 7. Red-shifted line from a point on a bright granule. The average profile shows a double bump.

Line profile of snapshot 2

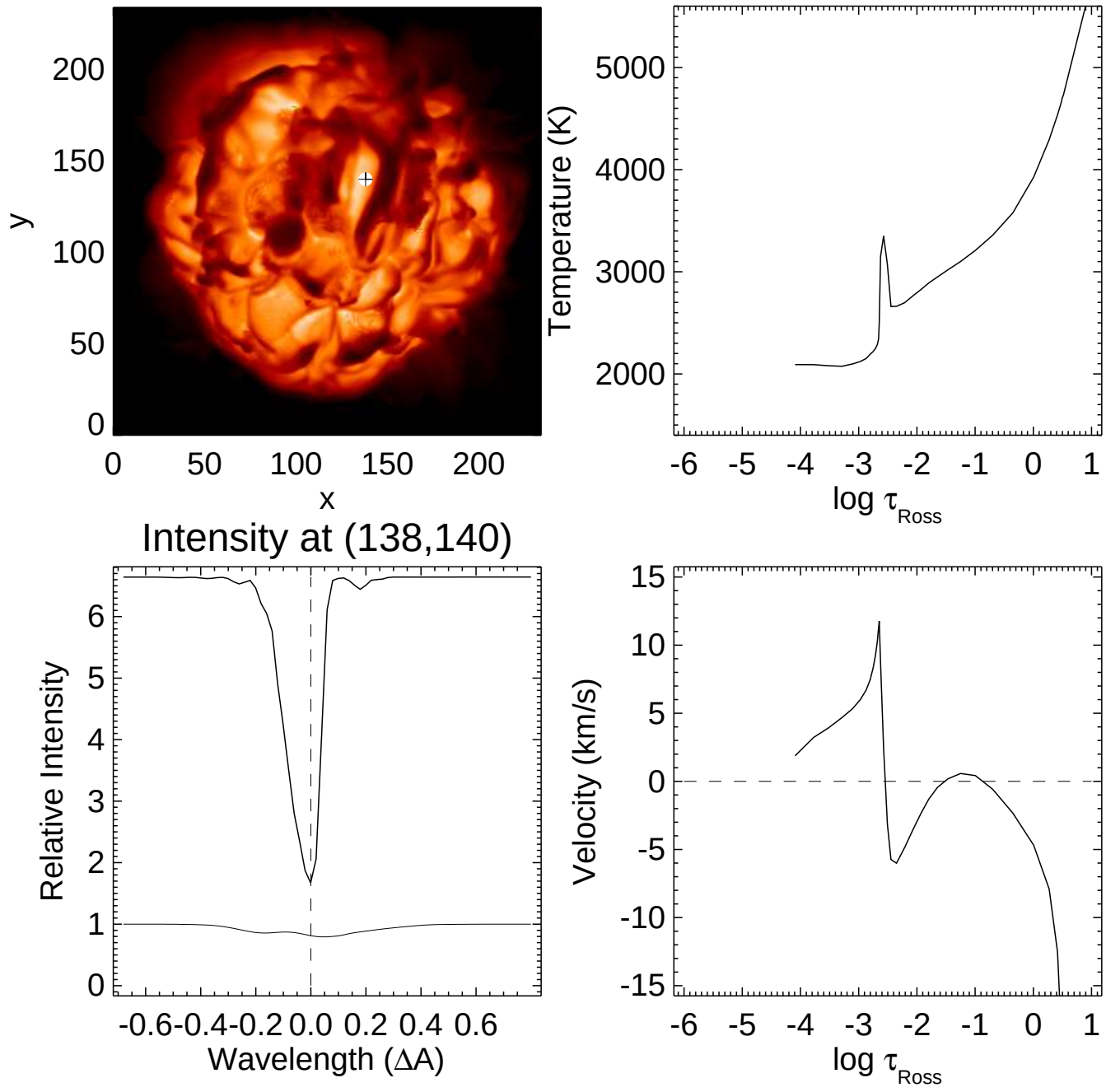

Figure 13: Sample line profile around 6219.281 Å: see Fig. 7. Slightly blue-shifted line from a point on a bright granule.

Line profile of snapshot 2

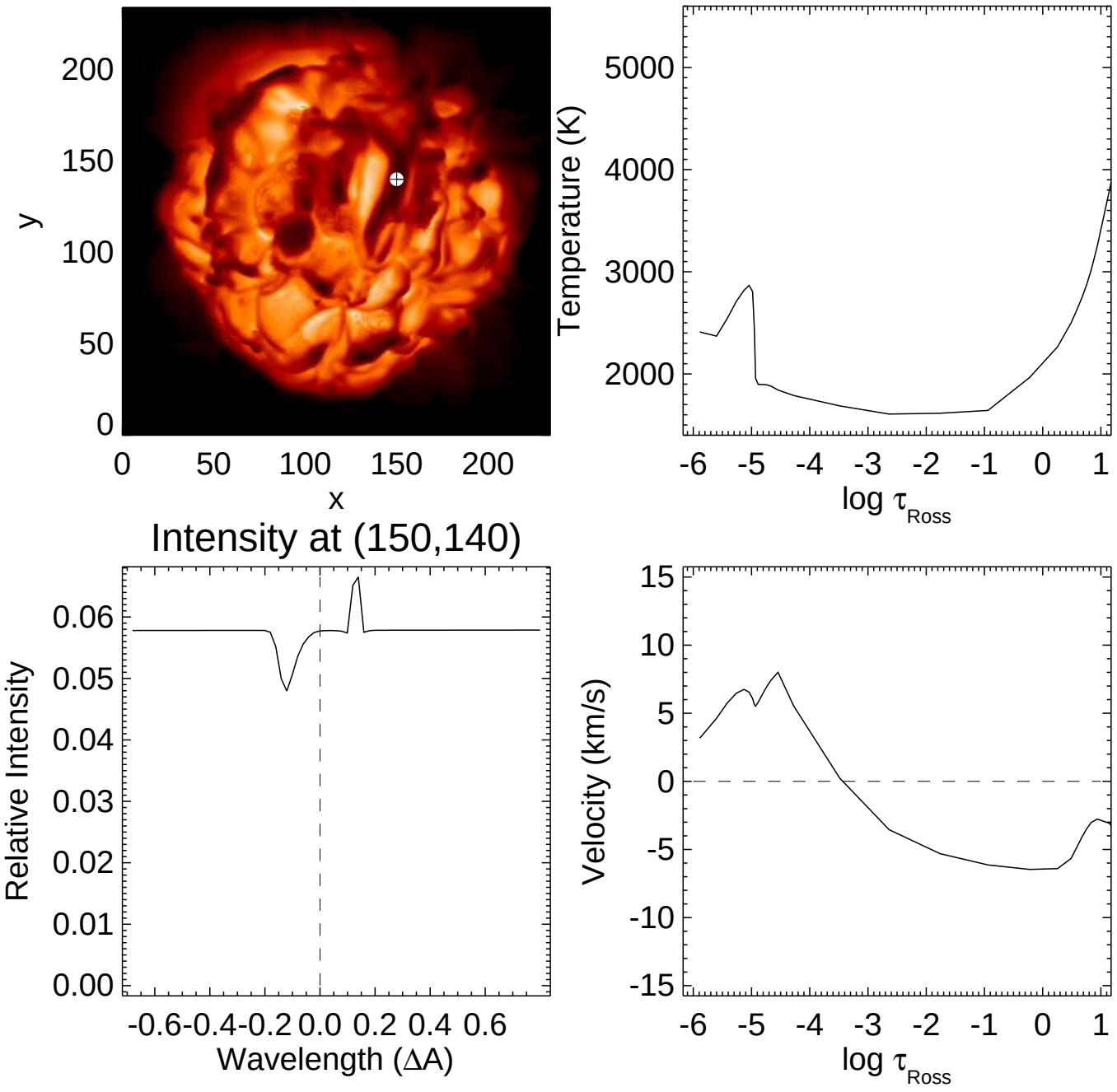

Figure 14: Sample line profile around 6219.281 Å: see Fig. 7. Weak line from intergranular region with emission-peak from shock. Note, that shock and granule are within regions with large-scale flows causing the non-trivial net Doppler shift.